Cluster expansion approach for transmutative lattice systems

2010 J. Phys.: Condens. Matter 22 125402

(http://iopscience.iop.org/0953-8984/22/12/125402)

IOP Publishing Journal of Physics: Condensed Matter

J. Phys.: Condens. Matter **22** (2010) 125402 (9pp) doi:10.1088/0953-8984/22/12/125402

Cluster expansion approach for transmutative lattice systems

Koretaka Yuge

Department of Materials Science and Engineering, Kyoto University, Sakyo, Kyoto 606-8501, Japan

Received 18 November 2009, in final form 29 January 2010
Published 8 March 2010
Online at stacks.iop.org/JPhysCM/22/125402

Abstract

We propose a cluster expansion (CE) technique that can express any function of atomic arrangement on any given lattice with the same number of lattice points in a single formalism. In the proposed CE, two types of spin variable, σ and τ, on the base lattice and virtual lattice, respectively, are introduced. The former spin variable specifies the occupation of the constituent elements for each lattice point. The latter specifies the positions of each lattice point. Basis functions constructed from the two types of spin variable satisfy completeness and orthonormality for any atomic arrangement on given lattices. As examples, the proposed CE is applied to one- and three-dimensional lattices in a binary system, which clarifies the concept of base and virtual lattices, how the functions of atomic arrangements are expressed in terms of the two types of spin variable, and the efficiency and convergence of the proposed CE with a finite number of clusters and input structures.

1. Introduction

Alloys exhibit a variation in their physical properties such as hardness, electric resistance, chemical reactivity and catalytic properties with changes in their constituent atomic arrangement and composition. The theoretical prediction of alloy configurational thermodynamics is a fundamental and important prerequisite to the design of desirable alloy materials in terms of narrowing down the controlling parameters. In particular, the recent increase in computational power has enabled us to predict the energetic of alloys through first-principles calculations based on density functional theory (DFT). However, the modeling of alloy thermodynamics requires the energetic for a tremendous number of atomic arrangements (in principle, R^N arrangements for R components on N lattice points), which still makes it difficult to directly apply DFT. Therefore, alternative approaches for predicting alloy thermodynamics has been proposed to reduce the computational load of DFT. The most promising and well-established approach is the cluster expansion [1, 2] (CE) technique, where the alloy energetics are described by the Ising-like Hamiltonian. The CE technique combined with DFT total energy calculation has been widely applied to predict a variety of aspects of alloy thermodynamics such as binary [3–7] and multicomponent [8–11] bulk phase diagrams, the prediction of ground-state structures [12], surface segregation and ordering [13–18], and the effects of lattice vibration [19, 20] and external pressure [21] on alloy phase stability. Furthermore, the CE formalism has been modified in various ways so that it can be applied to systems that practically require specific treatment in terms of the configuration spaces. Mixed-space CE [22–24], which treats clusters in both real and reciprocal space, has been applied to long-period superlattices, coupled CE [26], which treats distinct sublattices, has been applied to ionic systems and adsorption-induced surface segregation, and tensorial CE [25] can predict tensor-valued properties including dielectric constants and elasticity. Another modification of the CE technique is the procedure used to select optimized clusters and DFT input structures to increase the accuracy of predicted energies [12].

In spite of such successful applications of CE, there still remains an essential limitation preventing the modeling of more general alloy configurational thermodynamics. Although the CE formalism certainly allows us to estimate the energy of any atomic arrangement on a lattice with the desired accuracy, it is limited to the given lattice; different lattices require different expressions for the energy. This makes it difficult to apply CE to energetics for specific systems whose lattice points vary with changes in their circumstances such as temperature, atomic arrangement and composition. One can easily find such systems, which include graphite-like layered boron–carbon nitride, the shear structure of titanium oxide, polymorphous

silicon carbide and the close-packed alloy surface between fcc and hcp structures.

In the present paper, we propose a CE formalism, variable lattice CE (VLCE), which can overcome the above limitation of CE. In the following sections, we first derive the conventional CE formalism briefly and then explain the concept of the proposed VLCE and derive its formalism. We then consider a simple example of the application of VLCE to one-dimensional lattices with line and zigzag shapes, and clarify how effective interactions in VLCE can be interpreted intuitively. Finally, VLCE is applied to three-dimensional lattices with fcc and hcp structures to demonstrate how base and virtual lattices are introduced and how functions of atomic arrangements are expressed.

2. Expansion formalism for configuration functions

2.1. Conventional cluster expansion formalism

First, the formalism in conventional CE is explained to illustrate the basic concept of CE. Here we consider a single-crystalline system with N well-defined lattice points for the R component. The occupation of lattice point i ($i = 1 \cdots N$) by atomic element r ($r = 1 \cdots R$) is described by introducing the so-called spin variable σ_i, which takes different values for different r. Any atomic arrangement on the lattice points can be uniquely specified by an N-dimensional vector $\vec{\sigma} = \{\sigma_1, \sigma_2, \ldots, \sigma_N\}$. In CE, any function f that depends on the atomic arrangement is typically expanded in terms of the orthonormal basis functions of the atomic arrangement $\vec{\sigma}$, which are called cluster functions Ψ:

$$f(\vec{\sigma}) = \sum_w \langle f(\vec{\sigma})|\Psi_w(\vec{\sigma})\rangle \Psi_w(\vec{\sigma}), \tag{1}$$

where $\langle\,|\,\rangle$ denotes the inner product defined in $\vec{\sigma}$ space [1]. The basis functions $\{\Psi_w\}$ are constructed from the orthonormal basis $\{\rho\}$ at individual lattice points. The set $\{\rho\}$ is typically obtained by applying the following Gram–Schmidt technique to the linearly independent polynomial set $\{1, \sigma_i, \sigma_i^2, \ldots, \sigma_i^{R-1}\}$:

$$\begin{aligned} \rho_m(\sigma_i) &= \frac{b_m(\sigma_i)}{\langle b_m(\sigma_i)|b_m(\sigma_i)\rangle^{1/2}} \\ b_m(\sigma_i) &= \sigma_i^m - \sum_{j=0}^{m-1} \langle \rho_j(\sigma_i)|\sigma_i^m\rangle \rho_j(\sigma_i) \qquad (m \neq 0) \\ b_m(\sigma_i) &= 1 \qquad (m = 0), \end{aligned} \tag{2}$$

where m takes integer values of $0 \cdots R-1$. In this procedure, ρ_0 is always unity. Orthonormal basis functions for all N lattice points, Ψ, can thus be obtained by

$$v : \{\Psi(\vec{\sigma})\} = v : \{\rho(\sigma_1)\} \otimes \cdots \otimes v : \{\rho(\sigma_N)\}, \tag{3}$$

where $v:\{\chi\}$ denotes the vector space consisting of the set of functions χ. Note that, from equations (2) and (3), it is evident that two sets of indices are required to specify the cluster function Ψ: one is a set of lattice points, $\{i, j, \ldots k\}$, and the other is a set of indexed basis functions represented by a subscript ρ in equations (2). Therefore, any function f with atomic arrangement $\vec{\sigma}$ in equation (1) should be rewritten as follows:

$$\begin{aligned} f(\vec{\sigma}) &= \langle \Psi_0|f(\vec{\sigma})\rangle \Psi_0 + \sum_\alpha \sum_{(M)} \langle \Psi_\alpha^{(M)}(\vec{\sigma})|f(\vec{\sigma})\rangle \Psi_\alpha^{(M)}(\vec{\sigma}) \\ \Psi_\alpha^{(M)}(\vec{\sigma}) &= \rho_{d_1}(\sigma_i)\rho_{d_2}(\sigma_j)\cdots\rho_{d_n}(\sigma_k), \end{aligned} \tag{4}$$

where α specifies the set of lattice points whose basis function is not unity (i.e. $\neq\rho_0$), which corresponds to the n-body cluster consisting of lattice points $\{i, j, \ldots, k\}$, and (M) specifies the set of indexed basis functions in equations (4), $\{d_1, d_2, \ldots, d_n\}$. In equations (4), the function f is expanded exactly when the summations over α and (M) are performed over all possible clusters on the N lattice points and all possible combination of the indexes ρ, respectively. In practice, the expansion is truncated at a finite order owing to the limitation on the number of DFT input structures. The expansion coefficient, $\langle \Psi_\alpha^{(M)}(\vec{\sigma})|f(\vec{\sigma})\rangle$, is called the effective cluster interaction (ECI) for cluster α with index set (M). $\Psi_0 =$ unity is independent of $\vec{\sigma}$ and the corresponding cluster is called an empty cluster that has no explicit cluster figure. It is clear that conventional CE cannot treat the function f on different lattices in a single formalism since spin variable σ_i itself does not contain any information about the position of lattice point i. Thus, ECIs should be estimated on individual lattices.

2.2. Present treatment of cluster expansion

We first derive a VLCE expression that can treat any atomic arrangement on any well-defined lattice with N lattice points and R components. In order to treat a number of different lattices using a method on CE, we introduce two types of spin variable and two types of lattice. The first lattice is a 'base lattice', which has the same number of lattice points as the well-defined lattice, where the positions of the lattice points can be artificially determined. Each lattice point i is occupied by one of the R constituent components specified by the spin variable σ_i, in a similar fashion to conventional CE. Note that any artificially defined position for a base lattice point is amenable to VLCE, although the practical efficiency certainly depends on its definition. The second lattice is a 'virtual lattice', which also has the same number of lattice points as the well-defined lattice. Since the base, virtual and well-defined lattices have the same number of lattice points N, we give the same labels to the N lattice points of each lattice, $1 \cdots N$. Each lattice point i on the virtual lattice has one spin variable τ_i, which specifies the relative position of the corresponding well-defined lattice point i measured from the base lattice point i. Note that, since τ specifies the position of the well-defined lattice point, a combination of base lattice and τs can describe lattices whose positions of lattice points are essentially different from those on the base lattice. This definition of τ_i, i.e., the actual difference in position from the base lattice or the artificially normalized position, does not essentially alter the final VLCE expression obtained. For three-dimensional lattices, it is clear

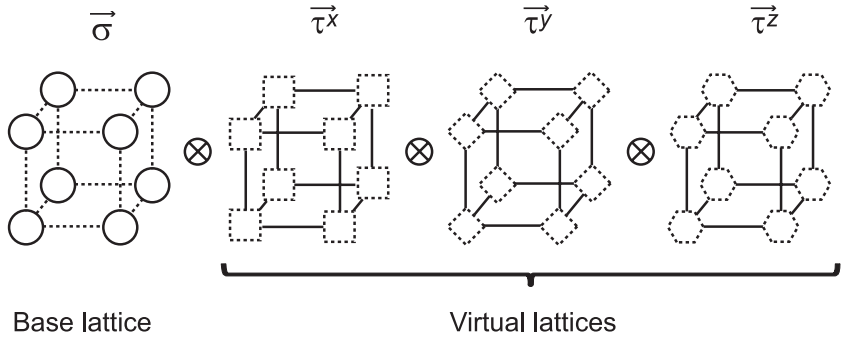

Figure 1. Schematic illustration of coupling between base and three virtual lattices for the x, y and z directions in cubic cells, which results in the atomic arrangement on any lattice consisting of eight lattice points.

that three spin variables, $\vec{\tau}_i = \{\tau_i^x, \tau_i^y, \tau_i^z\}$, are required to specify the position of lattice point i in Cartesian coordinates. Note that, while σ_i for the base lattice takes R values, the number of values that τ_i^η takes, R_η ($\eta = x$, y or z), depends on the number of positions in the lattices being considered. Figure 1 shows a schematic illustration of the coupling between the base lattice and the three virtual lattices that specify the positions of well-defined lattice points in the x, y and z directions in cubic cells. This results in the atomic arrangement on any lattice consisting of eight lattice points. Then any atomic arrangement on a well-defined lattice is uniquely specified by the $4N$-dimensional vector $\{\vec{\sigma}, \vec{\tau}\} = \{\sigma_1, \ldots, \sigma_N, \tau_1^x, \ldots, \tau_N^x, \tau_1^y, \ldots, \tau_N^y, \tau_1^z, \ldots, \tau_N^z, \}$. Orthonormal basis functions for a single lattice point i on a base or virtual lattice can be constructed from equations (2), which satisfy

$$\begin{aligned}
&\langle \rho_d(\sigma_i) | \rho_{d'}(\sigma_i) \rangle = \xi_{\text{base}}^N \text{Tr}_{\text{base}}^N \rho_d(\sigma_i) \rho_{d'}(\sigma_i) \\
&\quad = R^{-1} \sum_{\sigma_i} \rho_d(\sigma_i) \rho_{d'}(\sigma_i) = \delta_{dd'} \\
&\langle \rho_d(\tau_p^\eta) | \rho_{d'}(\tau_p^\eta) \rangle = \xi_\eta^N \text{Tr}_\eta^N \rho_d(\tau_p^\eta) \rho_{d'}(\tau_p^\eta) \\
&\quad = R_\eta^{-1} \sum_{\tau_p^\eta} \rho_d(\tau_p^\eta) \rho_{d'}(\tau_p^\eta) = \delta_{dd'}
\end{aligned} \tag{5}$$

for a single lattice point. Here, ξ_{base}^N and ξ_η^N are the normalized constants for the inner product of base and virtual lattice points, and $\text{Tr}_{\text{base}}^N$ and Tr_η^N are the trace operator on the $\vec{\sigma}_i$ and $\vec{\tau}_p^\eta$ space, respectively. Orthonormal basis functions for all lattice points on the base and virtual lattices, Φ, can then be obtained from

$$\begin{aligned}
&v : \{\Phi(\vec{\sigma}, \vec{\tau})\} = v : \{\Gamma_{\text{base}}(\vec{\sigma})\} \otimes v : \{\Xi_{\text{virtual}}(\vec{\tau^x})\} \\
&\qquad \otimes\ v : \{\Xi_{\text{virtual}}(\vec{\tau^y})\} \otimes v : \{\Xi_{\text{virtual}}(\vec{\tau^z})\} \\
&v : \{\Gamma_{\text{base}}(\vec{\sigma})\} = v : \{\rho(\sigma_1)\} \otimes \cdots \otimes v : \{\rho(\sigma_N)\} \\
&v : \{\Xi_{\text{virtual}}(\vec{\tau^\eta})\} = v : \{\rho(\tau_1^\eta)\} \otimes \cdots \otimes v : \{\rho(\tau_N^\eta)\},
\end{aligned} \tag{6}$$

where Γ_{base} and Ξ_{virtual} denote the orthonormal basis functions for the base and virtual lattices, respectively. Therefore, any function of an atomic arrangement for any lattice can be generally expressed as

$$\begin{aligned}
f(\vec{\sigma}, \vec{\tau}) &= \langle \Phi_0 | f(\vec{\sigma}, \vec{\tau}) \rangle \Phi_0 \\
&+ \sum_\alpha \sum_{(M)} \langle \Phi_\alpha^{(M)}(\vec{\sigma}) | f(\vec{\sigma}, \vec{\tau}) \rangle \Phi_\alpha^{(M)}(\vec{\sigma}) \\
&+ \sum_\eta \sum_\beta \sum_{(L_\eta)} \langle \Phi_\beta^{(L_\eta)}(\vec{\tau^\eta}) | f(\vec{\sigma}, \vec{\tau}) \rangle \Phi_\beta^{(L_\eta)}(\vec{\tau^\eta}) \\
&+ \sum_\eta \sum_{\alpha,\beta} \sum_{(M,L_\eta)} \langle \Phi_{\alpha;\beta}^{(M,L_\eta)}(\vec{\sigma}, \vec{\tau^\eta}) | f(\vec{\sigma}, \vec{\tau}) \rangle \Phi_{\alpha;\beta}^{(M,L_\eta)}(\vec{\sigma}, \vec{\tau^\eta}) \\
&+ \sum_{\eta \neq \eta'} \sum_{\beta,\beta'} \sum_{(L_\eta,L_{\eta'})} \langle \Phi_{\beta;\beta'}^{(L_\eta,L_{\eta'})}(\vec{\tau^\eta}, \vec{\tau^{\eta'}}) | f(\vec{\sigma}, \vec{\tau}) \rangle \\
&\times \Phi_{\beta;\beta'}^{(L_\eta,L_{\eta'})}(\vec{\tau^\eta}, \vec{\tau^{\eta'}}) \\
&+ \sum_{\eta \neq \eta'} \sum_{\alpha,\beta,\beta'} \sum_{(M,L_\eta,L_{\eta'})} \langle \Phi_{\alpha;\beta;\beta'}^{(M,L_\eta,L_{\eta'})}(\vec{\sigma}, \vec{\tau^\eta}, \vec{\tau^{\eta'}}) | f(\vec{\sigma}, \vec{\tau}) \rangle \\
&\times \Phi_{\alpha;\beta;\beta'}^{(M,L_\eta,L_{\eta'})}(\vec{\sigma}, \vec{\tau^\eta}, \vec{\tau^{\eta'}}) \\
&+ \sum_{\beta,\beta',\beta''} \sum_{(L_x,L_y,L_z)} \langle \Phi_{\beta;\beta';\beta''}^{(L_x,L_y,L_z)}(\vec{\tau^x}, \vec{\tau^y}, \vec{\tau^z}) | f(\vec{\sigma}, \vec{\tau}) \rangle \\
&\times \Phi_{\beta;\beta';\beta''}^{(L_x,L_y,L_z)}(\vec{\tau^x}, \vec{\tau^y}, \vec{\tau^z}) \\
&+ \sum_{\alpha,\beta,\beta',\beta''} \sum_{(M,L_x,L_y,L_z)} \langle \Phi_{\alpha;\beta;\beta';\beta''}^{(M,L_x,L_y,L_z)}(\vec{\sigma}, \vec{\tau^x}, \vec{\tau^y}, \vec{\tau^z}) | f(\vec{\sigma}, \vec{\tau}) \rangle \\
&\times \Phi_{\alpha;\beta;\beta';\beta''}^{(M,L_x,L_y,L_z)}(\vec{\sigma}, \vec{\tau^x}, \vec{\tau^y}, \vec{\tau^z}).
\end{aligned} \tag{7}$$

The inner product $\langle\, |\, \rangle$ is defined by

$$\langle g | h \rangle = \xi_0^{4N} \text{Tr}^{(4N)} g \cdot h, \tag{8}$$

where ξ_0^{4N} is the normalized constant of the inner product given by

$$\xi_0^{4N} = (R R_x R_y R_z)^{-N} \tag{9}$$

and $\text{Tr}^{(4N)}$ denotes the trace operator on the $\{\vec{\sigma}, \vec{\tau}\}$ space:

$$\text{Tr}^{(4N)} = \sum_{\sigma_1} \cdots \sum_{\sigma_N} \sum_{\tau_1^x} \cdots \sum_{\tau_N^x} \sum_{\tau_1^y} \cdots \sum_{\tau_N^y} \sum_{\tau_1^z} \cdots \sum_{\tau_N^z}. \tag{10}$$

The cluster functions Φ are given by

$$\begin{aligned}
\Phi_\alpha^{(M)} &= \prod_{\substack{I \in \alpha \\ d \in M}} \rho_d(\sigma_I) \\
\Phi_{\beta;\ldots\beta'}^{(L_\eta \ldots, L_{\eta'})} &= \prod_{\substack{P \in \beta \\ d \in L_\eta}} \rho_d(\tau_P^\eta) \cdots \prod_{\substack{P' \in \beta' \\ d' \in L_{\eta'}}} \rho_{d'}(\tau_{P'}^{\eta'}) \\
\Phi_{\alpha;\beta;\ldots\beta'}^{(M,L_\eta \ldots, L_{\eta'})} &= \prod_{\substack{I \in \alpha \\ d \in M}} \rho_d(\sigma_I) \prod_{\substack{P \in \beta \\ d' \in L_\eta}} \rho_{d'}(\tau_P^\eta) \cdots \prod_{\substack{P' \in \beta' \\ d'' \in L_{\eta'}}} \rho_{d''}(\tau_{P'}^{\eta'}).
\end{aligned} \tag{11}$$

The summations over α and β in equation (7) are taken over all possible clusters on the base and virtual lattices, and those over (M) and (L_η) are taken over all possible combinations of the basis function index for each lattice point on the base and virtual lattices for η, respectively. On the right-hand side of equation (7), the second term corresponds to the contribution from the base lattice; the third, fifth and seventh terms correspond to those from the virtual lattices; and the fourth, sixth and eighth terms correspond to those from the coupling between the base and virtual lattices.

ECIs for the VLCE can be obtained exactly by performing the inner products in equations (8)–(11), which require the values of $f(\vec{\sigma}, \vec{\tau})$ for all possible atomic arrangements on all possible lattices. In practice, an alternative approach can be introduced to estimate the ECIs through DFT calculations. Similarly to the conventional CE technique, the ECIs in VLCE can be estimated by taking a least-squares fitting, namely

$$\sum_s \{f_{\mathrm{DFT}}^{(s)} - f_{\mathrm{VLCE}}^{(s)}\}^2 = \min. \tag{12}$$

Here, $f_{\mathrm{DFT}}^{(s)}$ and $f_{\mathrm{VLCE}}^{(s)}$, respectively, denote the values of function f for the ordered structure s obtained via DFT calculation and via VLCE. The summation s is taken over a selected set of atomic arrangements on a number of lattices. Optimized DFT input ordered structures and clusters are typically determined by the genetic algorithm and the construction of a ground-state diagram [12].

In order to see the relationship between ECIs for conventional CE and for the proposed VLCE, we consider a single well-defined lattice whose arrangement on the virtual lattices is designated by $\vec{\tau_\gamma}$. Since $\vec{\tau_\gamma}$ is no longer a variable but a constant, we can obtain the following relationship by comparing equations (4) and (7) with $\vec{\tau} = \vec{\tau_\gamma}$:

$$\begin{aligned}
\langle \Psi_\alpha^{(M)}(\vec{\sigma})|f(\vec{\sigma})\rangle &= \langle \Phi_\alpha^{(M)}(\vec{\sigma})|f(\vec{\sigma},\vec{\tau_\gamma})\rangle \\
&+ \sum_\eta \sum_\beta \sum_{(L_\eta)} \langle \Phi_{\alpha;\beta}^{(M,L_\eta)}(\vec{\sigma},\vec{\tau_\gamma^\eta})|f(\vec{\sigma},\vec{\tau_\gamma})\rangle \Phi_\beta^{(L_\eta)}(\vec{\tau_\gamma^\eta}) \\
&+ \sum_{\eta\neq\eta'} \sum_{\beta,\beta'} \sum_{(L_\eta,L_{\eta'})} \langle \Phi_{\alpha;\beta;\beta'}^{(M,L_\eta,L_{\eta'})}(\vec{\sigma},\vec{\tau_\gamma^\eta},\vec{\tau_\gamma^{\eta'}})|f(\vec{\sigma},\vec{\tau_\gamma})\rangle \\
&\times \Phi_{\beta;\beta'}^{(L_\eta,L_{\eta'})}(\vec{\tau_\gamma^\eta},\vec{\tau_\gamma^{\eta'}}) \\
&+ \sum_{\beta,\beta',\beta''} \sum_{(L_x,L_y,L_z)} \langle \Phi_{\alpha;\beta;\beta';\beta''}^{(M,L_x,L_y,L_z)}(\vec{\sigma},\vec{\tau_\gamma^x},\vec{\tau_\gamma^y},\vec{\tau_\gamma^z})|f(\vec{\sigma},\vec{\tau_\gamma})\rangle \\
&\times \Phi_{\beta;\beta';\beta''}^{(L_x,L_y,L_z)}(\vec{\tau_\gamma^x},\vec{\tau_\gamma^y},\vec{\tau_\gamma^z}).
\end{aligned} \tag{13}$$

From equation (13), it is clear that the ECI for an α cluster on a well-defined lattice in conventional CE is described by the sum of the ECI corresponding to the α cluster on the base lattice and the ECIs corresponding to the coupling between the α cluster on the base lattice and all possible clusters on the virtual lattices.

While the general expression for VLCE given by equation (7) certainly describes the function on any given lattice, for real systems one can sometimes consider a restricted number of lattices. One of the most important examples is that lattices are described by a combination of positions of constituent lattices (hereinafter called partial lattices). In such specific cases, one can significantly reduce the number of terms in the expansion of equation (7) by introducing the following concepts. For simplicity, here we consider C lattices with N well-defined lattice points for R components, which are defined by differences in the one-dimensional positions of the constituent sublattices (i.e. one-dimensional stacking sequences). This consideration can be extended to two- and three-dimensional systems without loss of generality. One can easily find such examples including layered boron–carbon nitride, intercalation-dependent changes in the stacking sequence in graphite, hexagonal BN, the close-packed plane surface of fcc–hcp alloys (e.g. Al–Zn), composition-dependent one-dimensional stacking faults in Cu–Al, Cu–Sn and Au–Cd alloys, and chimney–ladder compounds of Ir-doped Mn–Si and Mn-doped Ru–Si. When all C lattices can be decomposed into the same combination of N' partial lattices, the N lattice points on the C lattices are completely specified by lattice points on the partial lattices and the positions of the partial lattices themselves. Note that we can consider any case of decomposition into partial lattices, i.e. (i) the number of lattice points on all the partial lattices is the same and the partial lattices are symmetry equivalent, (ii) the number of lattice points is the same but the partial lattices are not symmetry equivalent and (iii) the number of lattice points is not the same for each partial lattice. Therefore, instead of specifying all possible positions for the base lattice points, the spin variable τ_p is now defined to specify the position of each partial lattice p that takes R' values. Then the arrangements of the partial lattices can be expressed by a set of τ on a virtual lattice with N' lattice points. When the virtual lattice is successfully defined to describe all C lattices, any atomic arrangement on the N well-defined lattice points comprising these lattices is uniquely specified by the $(N + N')$-dimensional vector $\{\vec{\sigma}, \vec{\tau}\} = \{\sigma_1, \sigma_2, \ldots, \sigma_N, \tau_1, \tau_2, \ldots, \tau_{N'}\}$. In a similar fashion to the derivation of equation (7), we can immediately construct complete orthonormal basis functions for the C lattices using equations (2). Then any function of the atomic arrangement for the C crystalline systems can be expressed as

$$\begin{aligned}
f(\vec{\sigma},\vec{\tau}) &= \langle \Phi_0|f(\vec{\sigma},\vec{\tau})\rangle \Phi_0 \\
&+ \sum_\alpha \sum_{(M)} \langle \Phi_\alpha^{(M)}(\vec{\sigma})|f(\vec{\sigma},\vec{\tau})\rangle \Phi_\alpha^{(M)}(\vec{\sigma}) \\
&+ \sum_\beta \sum_{(L)} \langle \Phi_\beta^{(L)}(\vec{\tau})|f(\vec{\sigma},\vec{\tau})\rangle \Phi_\beta^{(L)}(\vec{\tau}) \\
&+ \sum_\alpha \sum_\beta \sum_{(M)} \sum_{(L)} \langle \Phi_{\alpha;\beta}^{(M,L)}(\vec{\sigma},\vec{\tau})|f(\vec{\sigma},\vec{\tau})\rangle \Phi_{\alpha;\beta}^{(M,L)}(\vec{\sigma},\vec{\tau}),
\end{aligned} \tag{14}$$

where

$$\begin{aligned}
\langle g|h\rangle &= \xi_0^{N;N'} \mathrm{Tr}^{(N;N')} g \cdot h \qquad \xi_0^{N;N'} = R^{-N} R'^{-N'} \\
\mathrm{Tr}^{(N;N')} &= \sum_{\sigma_1} \cdots \sum_{\sigma_N} \sum_{\tau_1} \cdots \sum_{\tau_{N'}}.
\end{aligned} \tag{15}$$

Thus, it is clear that the VLCE expression for lattices with a one-dimensional stacking sequence can be significantly simplified from the general expression of equations (7)–(14).

2.3. Classification of clusters according to symmetry

In the practical use of CE, the number of clusters or corresponding ECIs is typically reduced according to the symmetry of the lattice. In conventional CE, since the ECI $\langle \Psi_\alpha^{(M)}(\vec{\sigma})|f(\vec{\sigma})\rangle$ is independent of the atomic arrangement $\vec{\sigma}$, clusters α in the same set of basis indices (M) are classified with respect to the underlying empty lattice: all clusters with nonequivalent symmetry in class F are considered.

In VLCE, such a procedure to reduce the number of clusters becomes somewhat complicated because a number of lattices with different symmetries are simultaneously treated. From equation (7), the ECIs in VLCE are independent not only of atomic arrangement $\vec{\sigma}$ but also of the positions of lattice points or partial lattices, $\vec{\tau}$. The former does not change the symmetry of empty lattices, while the latter changes the symmetry of lattices. We emphasize here that the expansion of equation (7) is exact for any given set of lattices whose numbers of symmetry-equivalent clusters (e.g. $1-NN$ pair cluster) differ from each other. This is simply because information on all the symmetry operations for well-defined empty lattices is not essentially required to construct cluster functions in VLCE, which also holds true for conventional CE. Therefore, VLCE can treat different lattices whose numbers of equivalent symmetry clusters differ and its formalism in principle does not depend on the difference in the number of equivalent clusters. In order to reduce the number of clusters considered, several practical approaches can be proposed to classify the clusters. (i) All clusters are treated as being different, which always results in the rigorous expansion of equation (7). (ii) Clusters in intrapartial lattices and in virtual lattices are classified with the symmetry of the associated partial and virtual lattices. All clusters whose constituent lattice points belong to different partial lattices are treated as being different. (iii) Clusters in intra- and interpartial lattices are classified with the symmetry of one specific arrangement of the partial lattices. Note that several cluster classifications other than the above three should exist. In any case, invalid classification can sometimes severely violate the symmetry of the clusters used, which results in the slower convergence of ECIs or an incorrect estimation of the energy for specific atomic arrangements. Therefore, a suitable classification should be carefully considered, which depends on the given system. However, one can, in principle, obtain the desired accuracy in VLCE based on equation (7), since this expression rigorously satisfies a complete orthonormal expansion of function f. With these considerations, in section 3 we show an example of VLCE with no classification of clusters according to the symmetry.

3. Application of variable lattice cluster expansion

In this section, VLCE is applied to a specific system to demonstrate how base and virtual lattices are introduced, and how the function $f(\vec{\sigma},\vec{\tau})$ is actually expressed for individual systems. Also, we show how ECIs in VLCE are interpreted in terms of the preferences of corresponding clusters. In the following, we show the application of the simplified VLCE expression given by equation (14) for lattices that are described by a difference in their stacking sequences. This is because: (i) the general application of VLCE to any given lattice can always be achieved by equation (7) and (ii) in a similar fashion to the derivation of equation (14), one can modify the expression of VLCE to reduce the number of expansion terms of equation (7) by artificially defining partial lattices and a spin variable τ that are suitable for describing the desired set of lattices.

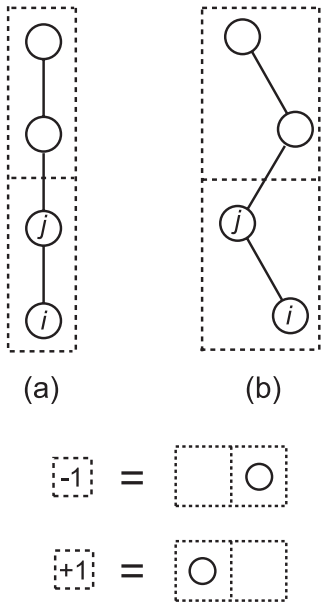

Figure 2. Upper figure: schematic illustration of one-dimensional lattices with (a) line and (b) zigzag shapes. The dashed rectangles represent the minimum unit of the lattice points used to distinguish the lattices in (a) and (b). i and j represent the lattice points. Lower figure: schematic illustration of the definition of the spin variable on the virtual lattice point in order to distinguish lattices with line and zigzag shapes. The left-hand side corresponds to the virtual lattice and the right-hand side represents positions of the partial lattices (here, lattice points i and j are denoted by solid circles).

3.1. One dimension: line and zigzag lattices

The first example we consider is the case of one-dimensional lattices with line and zigzag shapes, as respectively illustrated in the upper part of figures 2(a) and (b), in an A–B binary system. Although this is a simple example, its concept can be easily extended to real systems where the stacking sequence along one specific direction can vary with changes in the composition or atomic arrangement.

The dashed rectangles represent the minimum unit of the lattice points used to distinguish the lattices. Let us first derive a conventional CE expression for lattices (a) and (b). When we define the spin variables $\sigma_\theta = +1$ (-1) for the occupation of atom A (B) at lattice point θ $(\theta = i, j)$ on the well-defined lattice (a) or (b), the orthonormal basis functions at lattice point θ can be obtained through equations (2):

$$\rho_0(\sigma_\theta) = 1 \qquad \rho_1(\sigma_\theta) = \sigma_\theta. \tag{16}$$

Since one of the two basis functions is unity, the indices of the basis functions in equations (16) are not required to specify cluster functions. Thus, the cluster function is described by the

well-known expression

$$\Psi_\alpha = \prod_{\theta\in\alpha}\sigma_\theta. \tag{17}$$

Therefore, any function f on lattice (a) or (b) with two neighboring lattice points can be simply expressed in conventional CE as

$$f(\vec{\sigma}) = V^{\mathrm{r}}_0 + V^{\mathrm{r}}_{1-i}\sigma_i + V^{\mathrm{r}}_{1-j}\sigma_j + V^{\mathrm{r}}_{2-ij}\sigma_i\sigma_j, \tag{18}$$

where $V^{\mathrm{r}}_{\mu-\{\lambda\}}$ denotes the ECI for a μ-body cluster consisting of a set of lattice points $\{\lambda\}$ on the well-defined lattice (a) or (b). It is again clear that conventional CE cannot express the function f on lattices (a) and (b) simultaneously, since the spin variables σ_θ do not contain information to distinguish these lattices. Alternatively, $V^{\mathrm{r}}_{\mu-\{\lambda\}}$ in equation (18) depends on the lattices.

Next, we apply the VLCE technique to the one-dimensional lattices in figure 2. In order to treat lattices (a) and (b) by VLCE, we decompose the two lattices into two partial lattices, where one contains lattice point i and the other contains point j. Since the difference in lattices (a) and (b) can be well described by the difference in the stacking sequence, i.e. one atom on another atom with overhead position (lattice (a)) or to the left or right of the atom below position (lattice (b)) along the one-dimensional direction, the virtual lattice should have characters that specify the positions of partial lattices normal to the stacking direction: two positions for each partial lattice is sufficient to describe lattices (a) and (b). The lower side of figure 2 shows the possible corresponding virtual lattice point. We define the spin variable $\tau = +1$ (-1) on the virtual lattice by placing a partial lattice (here, lattice point i or j) on the left-(right)-hand side of the artificially introduced lattice, which is represented by the dashed lines on the right-hand side of the lower figure of figure 2. Then the well-defined lattices (a) and (b) in figure 2 can be expressed by coupling the base lattice and the virtual lattice with an explicit occupation as schematically illustrated in figure 3. Therefore, $\tau_p = \tau_q$ $(\tau_p \neq \tau_q)$ denotes lattice (a) with the line shape (lattice (b) with the zigzag shape).

Now we can express any function f on lattices (a) and (b) using spin variables σ and τ on the base and virtual lattices, namely:

$$\begin{aligned} f(\vec{\sigma},\vec{\tau}) = {} & V_0 + V^{\mathrm{b}}_{1-i}\sigma_i + V^{\mathrm{b}}_{1-j}\sigma_j + V^{\mathrm{b}}_{2-ij}\sigma_i\sigma_j \\ & + V^{\mathrm{v}}_{1-p}\tau_p + V^{\mathrm{v}}_{1-q}\tau_q + V^{\mathrm{v}}_{2-pq}\tau_p\tau_q \\ & + V^{\mathrm{b-v}}_{1-i;1-p}\sigma_i\tau_p + V^{\mathrm{b-v}}_{1-i;1-q}\sigma_i\tau_q + V^{\mathrm{b-v}}_{1-i;2-pq}\sigma_i\tau_p\tau_q \\ & + V^{\mathrm{b-v}}_{1-j;1-p}\sigma_j\tau_p + V^{\mathrm{b-v}}_{1-j;1-q}\sigma_j\tau_q + V^{\mathrm{b-v}}_{1-j;2-pq}\sigma_j\tau_p\tau_q \\ & + V^{\mathrm{b-v}}_{2-ij;1-p}\sigma_i\sigma_j\tau_p + V^{\mathrm{b-v}}_{2-ij;1-q}\sigma_i\sigma_j\tau_q \\ & + V^{\mathrm{b-v}}_{2-ij;2-pq}\sigma_i\sigma_j\tau_p\tau_q. \end{aligned} \tag{19}$$

Here, $V^{\mathrm{b}}_{\mu-\{\lambda\}}$ and $V^{\mathrm{v}}_{\mu-\{\lambda\}}$ denote the ECIs for a μ-body cluster consisting of a set of lattice points $\{\lambda\}$ on the base and virtual lattices, respectively, and $V^{\mathrm{b-v}}_{\mu-\{\lambda\};\mu'-\{\lambda'\}}$ denotes the ECI for the coupling of the μ-body cluster with lattice points $\{\lambda\}$ on the base lattice and the μ'-body cluster with lattice points $\{\lambda'\}$ on the virtual lattice. In contrast to the conventional CE formalism in equation (18), the VLCE formalism in equation (19) includes two types of spin variable, σ and τ, that can specify the atomic arrangements on both lattice (a) and lattice (b), and also the ECIs in equation (19) do not depend on the lattice type.

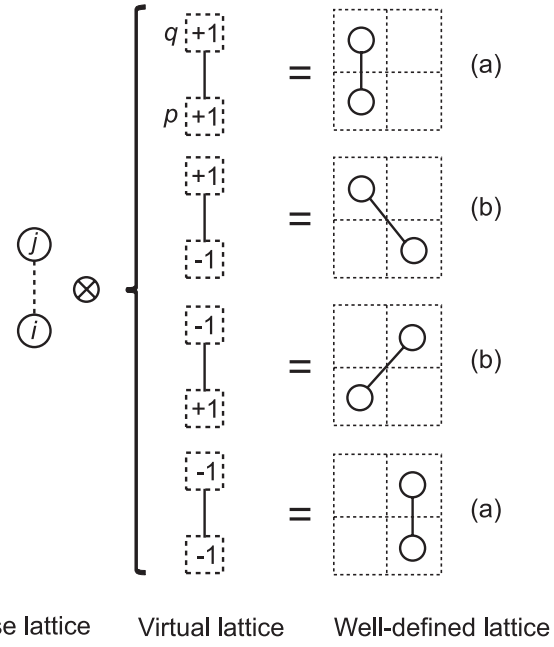

Figure 3. Schematic illustration of coupling of base lattice and virtual lattice with explicit occupation, resulting in two types of well-defined lattice (a) and (b) shown in figure 2.

From the above discussion, it is clear that the proposed VLCE can simultaneously treat functions on different lattices and how base and virtual lattices are introduced and their ECIs are actually expressed. Next, we investigate how the ECIs in VLCE are intuitively interpreted in terms of the preferences of constituent atoms in a certain cluster. For the well-used definition of the spin variable $\sigma = \pm 1$ on a well-defined lattice, conventional CE gives a clear interpretation of the ECIs for a pair cluster V^{r}_{2-ij}. When we take function f in equation (18) as the internal energy of a system for instance, $V^{\mathrm{r}}_{2-ij} > 0$ means the energetic preference for an unlike-atom pair between lattice points i and j, and $V^{\mathrm{r}}_{2-ij} < 0$ means that for a like-atom pair. Therefore, the signs of the ECIs for a pair cluster are a significant parameter related to the ordering tendency in a system.

In order to give a clear interpretation of the ECIs in VLCE, equation (13) is applied to a pair cluster on the base lattice. Then we obtain the relationship between the ECI for a pair cluster on the well-defined lattice and that for the base and virtual lattices:

$$V^{\mathrm{r}}_{2-ij} = V^{\mathrm{b}}_{2-ij} + V^{\mathrm{b-v}}_{2-ij;1-p}\tau_p + V^{\mathrm{b-v}}_{2-ij;1-q}\tau_q + V^{\mathrm{b-v}}_{2-ij;2-pq}\tau_p\tau_q. \tag{20}$$

When we rewrite the ECIs for a pair cluster on well-defined lattices (a) ($\tau_p = \tau_q = +1$ or $\tau_p = \tau_q = -1$) and (b) ($\tau_p = +1$, $\tau_q = -1$ or $\tau_p = -1$, $\tau_q = +1$) as $V^{\mathrm{r(a)}}_{2-ij}$ and $V^{\mathrm{r(b)}}_{2-ij}$,

respectively, these ECIs are explicitly expressed as

$$\begin{aligned} V^{\mathrm{r(a)}}_{2-ij} &= V^{\mathrm{b}}_{2-ij} + V^{\mathrm{b-v}}_{2-ij;1-p} + V^{\mathrm{b-v}}_{2-ij;1-q} + V^{\mathrm{b-v}}_{2-ij;2-pq} \\ &= V^{\mathrm{b}}_{2-ij} - V^{\mathrm{b-v}}_{2-ij;1-p} - V^{\mathrm{b-v}}_{2-ij;1-q} + V^{\mathrm{b-v}}_{2-ij;2-pq} \\ V^{\mathrm{r(b)}}_{2-ij} &= V^{\mathrm{b}}_{2-ij} + V^{\mathrm{b-v}}_{2-ij;1-p} - V^{\mathrm{b-v}}_{2-ij;1-q} - V^{\mathrm{b-v}}_{2-ij;2-pq} \\ &= V^{\mathrm{b}}_{2-ij} - V^{\mathrm{b-v}}_{2-ij;1-p} + V^{\mathrm{b-v}}_{2-ij;1-q} - V^{\mathrm{b-v}}_{2-ij;2-pq}, \end{aligned} \tag{21}$$

which naturally leads to

$$V^{\mathrm{b-v}}_{2-ij;1-p} = V^{\mathrm{b-v}}_{2-ij;1-q} = 0. \tag{22}$$

Therefore, the following relations can be derived from equations (21) and (22):

$$\begin{aligned} V^{\mathrm{r(a)}}_{2-ij} &= V^{\mathrm{b}}_{2-ij} + V^{\mathrm{b-v}}_{2-ij;2-pq} \\ V^{\mathrm{r(b)}}_{2-ij} &= V^{\mathrm{b}}_{2-ij} - V^{\mathrm{b-v}}_{2-ij;2-pq}. \end{aligned} \tag{23}$$

When we consider lattices (a) and (b) together, the most energetically favorable pair cluster is specified not only by the combination of the constituent elements but also by the arrangement of the partial lattices. The preference can be determined by the sign of the ECI for the pair cluster whose ECI exhibits the largest absolute value. For instance, $|V^{\mathrm{r(a)}}_{2-ij}| > |V^{\mathrm{r(b)}}_{2-ij}|$ and $V^{\mathrm{r(a)}}_{2-ij} < 0$ correspond to the preference for a like-atom pair on lattice (a). Thus, using equations (23) and by comparing the absolute value of ECIs for pair clusters on a well-defined lattice, we can construct a diagram of the most favorable pair clusters in terms of V^{b}_{2-ij} and $V^{\mathrm{b-v}}_{2-ij;2-pq}$ as shown in figure 4. Pair clusters consisting of an open circle and a closed circle denote unlike-atom pairs, and those consisting of two open or two closed circles denote like-atom pairs. Vertical clusters represent lattice (a) in figure 2 and slanted clusters represent lattice (b). The dotted axes represent the ECIs for the corresponding pair clusters on lattices (a) and (b). It can be clearly seen from figure 4 that four types of preferred pair cluster are reasonably characterized by the combination of signs of the ECI for the base lattice and that for the coupling of the base and virtual lattices. The line shape of lattice (a) is preferred when the signs of V^{b}_{2-ij} and $V^{\mathrm{b-v}}_{2-ij;2-pq}$ are the same, and the zigzag shape of lattice (b) is preferred when V^{b}_{2-ij} has a different sign from $V^{\mathrm{b-v}}_{2-ij;2-pq}$. A positive sign for V^{b}_{2-ij} results in the preference for an unlike-atom pair and a negative sign results in that for a like-atom pair.

Finally, we demonstrate practical applications of the VLCE including accuracy of the predicted energies for a number of lattices with a finite number of clusters used in order to see the efficiency and convergence of the VLCE. We employ all possible atomic arrangements on all possible one-dimensional lattices consisting of four lattice points under periodic boundary conditions constructed by base and virtual lattices as shown in figure 2. This results in 16 atomic arrangements on each of 16 lattices, i.e. 256 structures, where the number of corresponding clusters in VLCE should of course be 256 (i.e. 2^4 clusters on the base lattice times 2^4 clusters on the virtual lattice) that are complete and orthonormal to describe the 256 structures. Among the 256 structures, 31 structures are symmetry-distinct. In order to

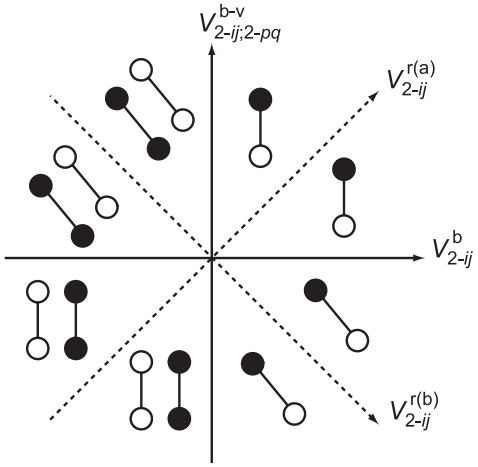

Figure 4. Diagram of the most favorable pair clusters in terms of V^{b}_{2-ij} and $V^{\mathrm{b-v}}_{2-ij;2-pq}$. Pair clusters consisting of an open circle and a closed circle denote unlike-atom pairs, and those consisting of two open circles or two closed circles denote like-atom pairs. Vertical clusters represent lattice (a) in figure 2 and slanted clusters represent lattice (b). The dotted axes represent the ECIs for the corresponding pair clusters on lattices (a) and (b).

treat these 31 structures, we take a low symmetry lattice where one of the four lattice points is located on the right (left)-hand side and the remaining three are on the left (right)-hand side, as the base lattice, and employ the virtual lattice in the line shape. In this case, a total of 54 VLCE clusters appear. Note that: (i) these 54 clusters are complete to describe the 31 structures. The reason why the number of clusters is larger than that of the structures is simply that the number of symmetry-nonequivalent clusters for a lower symmetry lattice should be larger than that for higher symmetry lattices, which naturally leads to splitting clusters for higher symmetry lattices. (ii) The number of clusters used in the VLCE thus certainly depends on the definition of base lattice. From (i) and (ii), it should be practically important to determine which lattice is taken as the base lattice: when we treat a set of higher symmetry lattices, the base lattice with lower symmetry could result in a number of unnecessary clusters. Meanwhile, when we treat a set of lower symmetry lattices, the base lattice with higher symmetry would cause a number of atomic arrangements on the lower symmetry lattice that cannot be distinguished.

We give above 54 clusters assumed ECIs, and then obtain energies for the 31 structures where variance of the energy is 0.43 eV/atom, the difference between maximum and minimum energy is 1.42 eV/atom and the minimum difference in energy is 0.02 eV/atom. Among the 31 structures, we make three sets of randomly selected 15 structures that are used to obtain ECIs through least-squares fitting of the given energies to the VLCE Hamiltonian. In order to estimate the accuracy of the fitted ECIs, a cross-validation (CV) score [27] is introduced. We search sets of a small number of clusters up to 11 clusters from the 54 clusters, which give the smallest CV score based on a genetic algorithm [28]. Figure 5 shows the resultant CV score as a function of the number of clusters. Closed circles, triangles and squares correspond to the three sets of 15 input structures. From figure 5, it is clear that,

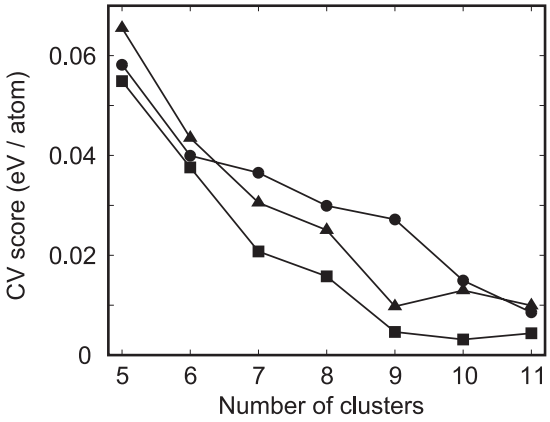

Figure 5. Smallest CV score as a function of the number of clusters used. Closed circles, triangles and squares correspond to three sets of 15 VLCE input structures.

for an appropriate selection of input structures (here, closed squares), nine clusters can reasonably predict relative energies with a low CV score below ∼0.01 eV/atom (i.e. half of the minimum difference in energy of 0.02 eV/atom for the given 31 structures). This result certainly indicates the practical efficiency of the proposed VLCE to predict energies for atomic arrangements on a number of lattices.

3.2. Three dimensions: fcc and hcp lattices

According to section 3.1, no special technique is required in VLCE to treat binary alloys on three-dimensional lattices described by one-dimensional stacking sequences. Here we consider fcc and hcp lattices that are well characterized by the stacking sequence of the close-packed plane (i.e. fcc is characterized by A–B–C–A–B–C–· · · and hcp is characterized by A–B–A–B–A–B–· · · stacking). The fcc and hcp lattices are first decomposed into partial lattices, each of which consists of a close-packed plane of fcc or hcp lattices. Then we define a spin variable on the virtual lattice to specify the position (stacking sequence) of the partial lattices: the spin variable with $\tau = +1$, $\tau = 0$ and $\tau = -1$ represent stacking types A, B and C, respectively. Then the well-defined fcc and hcp lattices can be expressed by coupling the base and virtual lattices as schematically illustrated in figure 6. Here, six partial lattices are used to distinguish the fcc and hcp lattices, resulting in six virtual lattice points of p–u. Therefore, we can express any function f on the fcc and hcp lattices by coupling the clusters with binary atomic arrangements on the base lattice and those with ternary partial lattice arrangements on the virtual lattice, namely

$$f(\vec{\sigma},\vec{\tau}) = V_0 + \sum_{\alpha}\left\{V_\alpha \prod_{I\in\alpha}\sigma_I\right\} + \sum_{\beta}\sum_{(L)}\left\{V_\beta^{(L)} \prod_{\substack{P\in\beta \\ d\in L}}\rho_d(\tau_P)\right\} + \sum_{\alpha}\sum_{\beta}\sum_{(L)}\left\{V_{\alpha;\beta}^{(L)} \prod_{I\in\alpha}\sigma_I \prod_{\substack{P\in\beta \\ d\in L}}\rho_d(\tau_P)\right\}, \quad (24)$$

where

$$\rho_1(\tau_P) = \sqrt{\tfrac{3}{2}}\tau_P \qquad \rho_2(\tau_P) = -\sqrt{2}(1-\tfrac{3}{2}\tau_P^2). \quad (25)$$

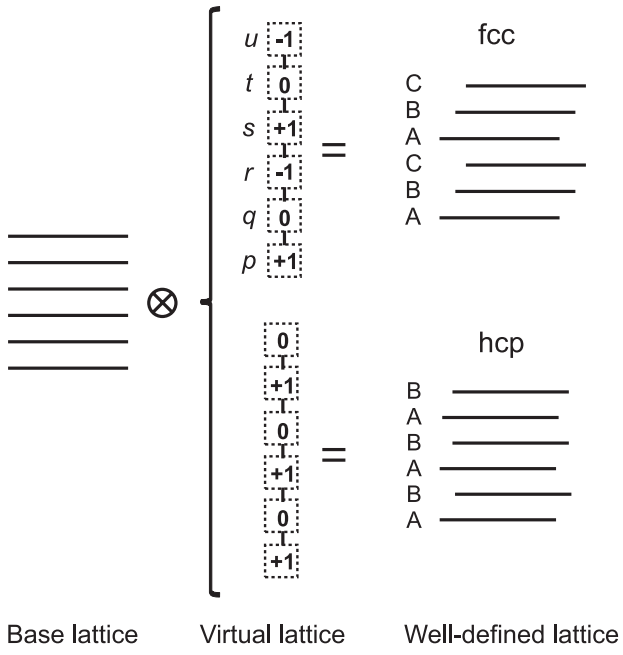

Figure 6. Schematic illustration of coupling of base lattice and virtual lattice, resulting in well-defined fcc and hcp lattices. Here, horizontal bold lines denote the close-packed plane of fcc or hcp lattices. Stacking types of fcc (ABCABC · · ·) and hcp (ABABAB · · ·) are described by spin variables of −1, 0 and +1 on virtual lattice, in a similar fashion to the definition of virtual lattice for one-dimensional line and zigzag lattices in section 3.1.

In equation (24), the summations over α and β are taken over all possible clusters consisting of base- and virtual lattice points, respectively. The summation over (L) is taken over all possible combinations of the basis function index corresponding to the dimensions of the clusters: since the virtual lattice has three values for the spin variable, two basis functions, ρ_1 and ρ_2 in equations (25), are required. These basis functions can be obtained via equations (2) [11]. Using equation (24), we can express the function f not only on fcc and hcp lattices but also on other lattices with different stacking sequences of the close-packed plane.

To summarize, we derived a VLCE formalism that can be applied to any atomic arrangement on any given lattice with the same number of lattice points. In the practical application of VLCE, one can reduce the number of clusters used and the number of lattices to be treated by decomposing well-defined given lattices into partial lattices and artificially introducing corresponding virtual lattices so that coupling of the base and virtual lattices can describe the desired lattices. Therefore, the definition of the base and virtual lattices and the partial lattices depend on the problem of interest and are not always unique.

4. Conclusions

We propose a cluster expansion technique, variable lattice cluster expansion (VLCE), which can treat any given lattice with the same number of lattice points in a single formalism. Two types of spin variable, σ on the base lattice and τ on the virtual lattice, are introduced to uniquely specify the atomic

arrangements on the lattices. The former specifies atomic arrangements on the base lattice and the latter specifies the positions of each base lattice point. Then any function of an atomic arrangement on the lattices can be rigorously expanded in terms of the complete and orthonormal basis functions constructed from the two types of spin variable. We also introduce the concept of partial lattices to effectively reduce the number of clusters used as well as the number of lattices considered. The given lattices are determined by the positions of the partial lattices, which are described by τ. To demonstrate how the base and virtual lattices are introduced, and how the ECIs in VLCE are interpreted, we first give a simple example of one-dimensional lattices with line and zigzag shapes. The signs of the ECIs on the base lattice and those for the coupling between the base and virtual lattices successfully enable an intuitive interpretation of which pair cluster is energetically favored in terms not only of the combination of constituent elements but also that of partial lattice arrangements. Using a finite number of ECIs extracted from a finite number of input structures, we demonstrate convergence of the VLCE, which indicates the practical efficiency to describe relative energetic for a number of atomic arrangements on given lattices. VLCE is then applied to three-dimensional fcc and hcp lattices, where they are described by a stacking sequence of a close-packed plane. Since VLCE can predict the properties of any atomic arrangement on a given lattice from those on different lattices, it has a significant advantage in enhancing the number of states that can effectively be explored through the CE technique in configuration space.

Acknowledgments

This research was supported by a Grant-in-Aid for Young Scientists Start-up (20860048). The author would like to express cordial thanks to Drs Yukinori Koyama and Kazuaki Toyoura of Kyoto University for a fruitful discussion about the proposed formalism.

References

[1] Sanchez J M, Ducastelle F and Gratias D 1984 *Physica* A **128** 334
[2] Sanchez J M and Becker J D 1993 *Mater. Res. Soc. Proc.* **291** 115
[3] Lu Z W, Wei S-H and Zunger A 1991 *Phys. Rev. Lett.* **66** 1753
[4] Asta M, de Fontaine D, van Schilfgaarde M, Sluiter M and Methfessel M 1992 *Phys. Rev.* B **46** 5055
[5] Walle A and Ceder G 2002 *J. Phase Equilib.* **23** 348
[6] Zarkevich N A and Johnson D D 2004 *Phys. Rev. Lett.* **92** 255702
[7] Curtarolo S, Morgan D and Ceder G 2005 *CALPHAD* **29** 163
[8] Wolverton C and de Fontaine D 1994 *Phys. Rev.* B **49** 8627
[9] Alonso P R and Rubiolo G H 2000 *Phys. Rev.* B **62** 237
[10] Lechermann F, Fähnle M and Sanchez J M 2005 *Intermetallics* **13** 1096
[11] Yuge K, Seko A, Koyama Y, Oba F and Tanaka I 2008 *Phys. Rev.* B **77** 094121
[12] Blum V, Hart G L W, Walorski M J and Zunger A 2005 *Phys. Rev.* B **72** 165113
[13] Ruban A V and Skriver H L 1999 *Comput. Mater. Sci.* **15** 119
[14] Drautz R, Reichert H, Fähnle M, Dosch H and Sanchez J M 2001 *Phys. Rev. Lett.* **87** 236102
[15] Pourovskii L V, Ruban A V, Johansson B and Abrikosov I A 2003 *Phys. Rev. Lett.* **90** 026105
[16] Yuge K, Seko A, Kuwabara A, Oba F and Tanaka I 2006 *Phys. Rev.* B **74** 174202
[17] Müller S, Stöhr M and Wieckhorst O 2006 *Appl. Phys.* A **82** 415
[18] Yuge K, Seko A, Kuwabara A, Oba F and Tanaka I 2007 *Phys. Rev.* B **76** 045407
[19] Garbulsky G D and Ceder G 1996 *Phys. Rev.* B **53** 8993
[20] Walle A and Ceder G 2002 *Rev. Mod. Phys.* **74** 11
[21] Yuge K 2009 *J. Phys.: Condens. Matter* **21** 055403
[22] Laks D B, Ferreira L G, Froyen S and Zunger A 1992 *Phys. Rev.* B **46** 12587
[23] Ozoliņš V, Wolverton C and Zunger A 1998 *Phys. Rev.* B **57** 6427
[24] Blum V and Zunger A 2004 *Phys. Rev.* B **70** 155108
[25] Walle A 2008 *Nat. Mater.* **7** 455
[26] Han B C, van der Ven A, Ceder G and Hwang B J 2005 *Phys. Rev.* B **72** 205409
[27] Walle A, Asta M and Ceder G 2002 *CALPHAD* **26** 539
[28] Hart G L W, Blum V, Walorski M J and Zunger A 2005 *Nat. Mater.* **4** 391